^{60}FE STUDIES WITH INTEGRAL'S SPECTROMETER SPI

W. Wang[1], M.J. Harris[1], R. Diehl[1], H. Halloin[2], C. Ciemniak[1], A.W. Strong[1], and K. Kretschmer[1]

[1] *Max-Planck-Institut für extraterrestrische Physik, Postfach 1603, 85740 Garching, Germany*
[2] *Fédération de Recherche APC, Collège de France, 11 Place Marcelin Berthelot, 75231 Paris, France*

ABSTRACT

The spectrometer SPI on board *INTEGRAL* has accumulated nearly three years' worth of data. We have analyzed these data to detect the γ-ray lines at 1173 and 1333 keV from ^{60}Fe, obtaining a precise measurement of both lines with 4.9 σ significance. The average flux per line is $\sim (4.4 \pm 0.9) \times 10^{-5}$ ph cm^{-2}s^{-1} from the inner Galaxy. With the same method and data, we derive a flux ratio of ^{60}Fe/^{26}Al $\sim 0.148 \pm 0.06$. We discuss the implications of these results for the widely-held hypothesis that ^{60}Fe is synthesized in massive stars.

1. INTRODUCTION

The isotope ^{60}Fe is one of several which are believed to be synthesized in massive stars, before or during their final evolution to core collapse supernovae (CCSN) and which survive to be detected afterwards by radioactive-decay and γ emission — ^{44}Ti, ^{56,57}Co, and ^{26}Al are other examples. They provide evidence that nucleosynthesis is ongoing in the Galaxy (with CCSN occurring at intervals $\sim$ 30–100 yr [25]), and will reveal many hidden details of such events. The species ^{44}Ti and ^{56,57}Co have relatively short half-lives ($\sim$ years) and are detected close to the immediate sources — the Type II supernova remnants Cas A and 1987A respectively [8], [11], [16]. With its much longer half-life ($\sim 10^6$ years), ^{26}Al accumulates in the interstellar medium (ISM) from many supernovae until ISM injection and β-decay are in balance, giving rise to a diffuse Galaxy-wide glow [15]. The behavior of ^{60}Fe should follow that of ^{26}Al, since its half-life is similar, $\sim 2 \times 10^6$ years.

The detection of ^{60}Fe promises to provide new information about these problems, in view of its massive star CCSN origin. RHESSI has reported the observations of the gamma-ray lines of ^{60}Fe with 2.6 σ, whose average flux is $\sim (3.6 \pm 1.4) \times 10^{-5}$ph cm^{-2} s^{-1} [23]. The analysis of the first year SPI data produced a marginal detection of γ-ray lines from ^{60}Fe ($\sim 3\sigma$, [6], with mean flux $\sim (3.7 \pm 1.1) \times 10^{-5}$ph cm^{-2} s^{-1}. The SPI spectrometer on board the *INTEGRAL* spacecraft has continued to collect data for two further years. We analyzed 2.5 years of data with the standard data processing and software developed in the Max-Planck-Institut für extraterrestrische Physik (MPE) Gamma group, expecting to obtain the more precise results from ^{60}Fe signals.

In the next section, we first introduce the observations of SPI. In §3, we describe the procedures and methods of data analysis. The scientific results, including the spectra and intensity of both 1173 keV and 1333 keV lines, and the flux ratio of ^{60}Fe/^{26}Al are presented in §4. The discussions and summary follow in §5.

2. OBSERVATIONS

The *INTEGRAL* spacecraft was launched on October 17, 2002 into a high-inclination, high-eccentricity orbit intended to avoid the increased background from the Earth's trapped radiation belts. The orbital period is 3 days. The spectrometer SPI consists of 19 Ge detectors actively shielded by a BGO anti-coincidence shield, with its aperture modulated by a tungsten coded mask which allows a high resolution imaging capability at $\sim 3°$ precision within a $16° \times 16°$ field of view (imaging on *INTEGRAL* is mainly performed at lower energies by the IBIS telescope, with which SPI is co-aligned). The Ge detectors, operating between 20 keV - 8 MeV, with a total effective area $\sim$ 70 cm^2 at 1 MeV, achieve an energy resolution $\sim$ 2.5 keV at 1 MeV [1], [22]. However, cosmic ray (CR) impacts degrade this resolution over time, and the instrument is periodically shut off for a few days while annealing (by heating from cryogenic temperatures to 100°C) is applied to the detectors to restore the energy resolution by removing the CR-induced defects [12], [22].

In operation IBIS and SPI are pointed at predesignated targets for intervals which vary but are typically $\sim$ 2000 *s* (referred to as *pointings* or *science windows*) which are often succeeded or followed by a

standard pattern of neighbouring pointings for imaging or survey purposes (*dithering* [9]).

The interval covered by the observations analyzed here is December 3, 2002 — August 22, 2005 (orbits 17–359). The instrument was in operation for most of this time, but important gaps were caused by five of the annealing episodes described above, and by the regular perigee passages with gaps due to the radiation belts. The live time was further reduced by the failure of two of the 19 detectors during this interval (December 2003 and July 2004) and by the occurrences of solar flares.

3. DATA ANALYSIS

The basic spectra per pointing are dominated by the intense background radiation characteristic of space platforms undergoing CR bombardment. Much of this radiation is prompt, resulting directly from CR impacts, whose variation with time ought to follow that of the incident CR flux. Another component arises from radioactive isotopes produced by the CR impacts whose decay lifetimes are relatively long. These isotopes will increase in abundance until CR production balances β-decay. A time series of their γ-ray emission will be the convolution of the time behavior of the prompt CR source with an exponential decrease from decay. The background continuum and the short-lived radioactive lines (i.e. $\leq$ the characteristic length of a science window) should follow the prompt CR time variability, while the many lines from longer-lived isotopes will have the second kind of temporal behavior.

The weak underlying celestial source of ^{60}Fe lines will have a different time signature, depending only upon how its exposure to the SPI aperture changes as one pointing succeeds another. We therefore extract the time series of count rates in each detector, in all science windows, and in predefined energy bins, and fit each to the sum of the time series of expected count rates for the several components of the background, plus the time series of count rates expected from the source as exposed to SPI. The amplitude of this last term in the fit is taken to be the count rate from the celestial source.

3.1. Background treatments

The background components listed above may exhibit complex time series which are derived from more than one physical source. We searched for such combinations, which, if they proved satisfactory, we adopted as *templates*. We tested several possible proxies for the source term of prompt CR excitation, including the rates measured in SPI's plastic scintillator anticoincidence detector, the rate of saturated events in the BGO shield, and the detector-by-detector rate of saturated events in the Ge detectors themselves (hereafter referred to as GEDSAT). The last of these, corresponding to events depositing >8 MeV, was found to perform this function best.

The most important radioactive background component is the line emission from ^{60}Co in the instrument, whose two lines at 1173 and 1333 keV are actually part of the ^{60}Fe decay chain. The convolution of the GEDSAT tracer with the exponential function $e^{-t/\tau}$, in which the decay time is that of ^{60}Co (7.6 yr), is expected to be a component of the templates for energy bins containing contributions from these lines, i.e. around 1173 and 1333 keV. A second possible radioactive contaminant may be the strong ^{69}Ge K-shell electron capture line (1337 keV) which is blended with the 1333 keV ^{60}Fe line. Its lifetime is 2.35 days. Because the decay time is short, the convolution of the GEDSAT tracer with the exponential function (τ = 2.35 days) is similar to the GEDSAT tracer itself, then we just take the GEDSAT as a background component tracer for this strong instrumental line feature.

3.2. Analysis procedure

A suite of software tools has been developed by the MPE team to implement such analysis of SPI data. They perform the following operations in sequence:

(a) Data selection and combination: *spiselectscw*
Here the science windows during revolutions $17-359$ are tested for data quality. Most of the tests verify that the count rates in several onboard radiation detectors do not exceed limits, e.g. the INTEGRAL Radiation Environment Monitor [5]), the plastic scintillator anticoincidence counter (PSAC), the digital front end electronics, and GEDSAT (see §3.1), but also include instrument status codes, data ownership, and portions of the orbit phase (0.05–0.95). The science window data (events, dead times, good time intervals, pointings etc.) are assembled.

The selected data include counts of single events (SE) and multiple events (ME). The energy binning for our analysis is 1 keV in $\sim$ 20 keV intervals around and including the lines. The energy range extends between 1153 - 1193 keV and 1313 - 1359 keV. We also select energy bands on the higher and lower sides of each line for background modelling, from which the adjacent continuum's time behavior is to be determined (for example: 1163 - 1169 keV plus 1177 - 1184 keV and 1318 - 1328 keV plus 1349 - 1359 keV). We applied the *spiselectscw* operations including the selection criteria described above from orbits 17 to 359. The total time for the observations is $\sim$ 24 Ms.

(b) background modelling: *spiorthomodel*
The time series of the detector-by-detector count

rates in the four continuum bands are fitted by one or more tracers of prompt irradiation. If more than one, they are resolved into orthogonal components whose amplitudes indicate their relative importance (see §3.1). For more details on the orthogonalized background modelling, see related earlier papers [3], [4]. In the first step, we want to create the continuum background template from the adjacent energy band data. We found the best adjacent template to be a simple one formed from the GEDSAT time series defined above together with a constant. Secondly, for the 1 keV bin data for the science analyses, we found the best template to be a relatively simple one, comprising three templates: the adjacent continuum template, GEDSAT, and GEDSAT convolved with a 7.6 yr exponential for the radioactive build-up.

(c) Model fitting and spectra: *spimodfit*
The program *spimodfit* uses the binned count data, pointing and exposure information, and the instrumental response, to fit sky models (diffuse emission), point sources and background [24]. The output is in the form of FITS files containing, for all processed energies: the fit parameters, the covariance matrices and the input models. The counts per energy bin, per detector, and per pointing are fitted to the templates described in (b) and the time series of exposures with the SPI aperture of an assumed sky map of ^{60}Fe distribution. The count data for the spectra are modelled as:

$$D_{e,d,p} = A^{m,n}_{e,d,p}\beta_s I^{m,n} + F(B_{e,d,p}) + \delta_{e,d,p}, \qquad (1)$$

where *e,d,p* are indices for data space dimensions: energy, detector, pointing; *m,n* indices for the sky dimensions (galactic longitude, latitude); A is the instrument response matrix, I is the intensity per pixel on the sky. The background model function includes three components: $F(B_{e,d,p}) = \beta_1 \cdot Adjacent + \beta_2 \cdot GeDSat + \beta_3 \cdot GeDSat_{conv}$, where $Adjacent, GeDSat$ and $GeDSat_{conv}$ denote three background templates described in (b) respectively. Coefficients β_s for the sky map intensity (constant in time) and $\beta_{1,2,3}$ for three background intensities (time variation allowed) are derived, and the amplitude β_s comprises the resultant spectra of the signal from the sky. δ is the residue after the fitting. Generally, a good background model will lead to residuals fluctuations (within error bars) around zero.

The fits were performed for the three intervals December 2002 — December 2003, December 2003 — July 2004, and July 2004 — August 2005, corresponding to the different sets of active detectors (§2). Separate fitting was made for each of the Fe lines and for SE and ME respectively. From the combined results, the amplitude of the ^{60}Fe emission for the map adopted was obtained. The map of ^{26}Al Galactic distribution from the 9-year data of COMPTEL [18] was taken to be the standard sky distribution model, but we have also compared the results with those of several other maps.

Table 1. ^{60}Fe intensity in the inner Galaxy

	Flux (10^{-5} ph cm^{-2} s^{-1})
1173 keV (SE)	4.1 ± 1.8
1173 keV (ME)	4.1 ± 2.4
1333 keV (SE)	3.8 ± 1.8
1333 keV (ME)	5.9 ± 2.4

4. RESULTS

By fitting the SE and ME data sets of observations at 1 keV wide energy binning independently, with the sky intensity distribution of ^{26}Al image by 9-year COMPTEL observations together with the background model based on the orthogonalized background tracers, we can obtain the spectra of two lines (1173 keV and 1333 keV) of ^{60}Fe emission from the Galaxy. Thus we obtain four spectra from *spimodfit* (§3.2 c) shown in Figure 1. We then fit these spectra with a spectral model consisting of a continuum, and spectral lines with profiles as expected from the variations of SPI spectral response (§2). We apply Gaussian profiles with aa fixed width of ~ 2.76 keV which is derived from adjacent instrumental line-shape fitting (e.g. the instrumental line at 1107 keV). The ^{69}Ge line at 1337 keV has also been eliminated well (about a fact of 4 compared with Harris et al. [6]). Yet, this strong instrumental line leads to a peculiar spectral signature which clearly is recognized as an artifact and not confused with the celestial line.

In Figure 1, we present four spectra: two lines (1173 keV and 1333 keV) of ^{60}Fe for both SE and ME databases. Intensity is given in relative units of sky map coefficients. The total line flux for each line is determined from the normalization of the input sky map intensity for the inner Galaxy region (e.g. $-30° < l < 30°$, $-10° < b < 10°$). We show line fluxes of two ^{60}Fe lines for the SE and ME data in Table 1, respectively. All line flux values are consistent within uncertainties.

The astrophysical signal of ^{60}Fe lines is very weak, the detection in each of our four spectra is marginally significant ($< 3\sigma$). Therefore, we cannot determine line shape information as we have done for the ^{26}Al line [3]. Here we fit the data points only with fixed width, which is based on the SPI instrumental line width around 1100 keV. The fits appear satisfactory, suggesting that the celestial ^{60}Fe lines are also intrinsically-narrow lines, similar to the observed ^{26}Al line from the inner Galaxy [3] (also see Fig. 2).

As mentioned in §3.2 (c), we determined the spectra from model fitting, which is dependent on the input sky map (also see Eq. 1). We do not know the real distribution of ^{60}Fe sources in the Galaxy, but we

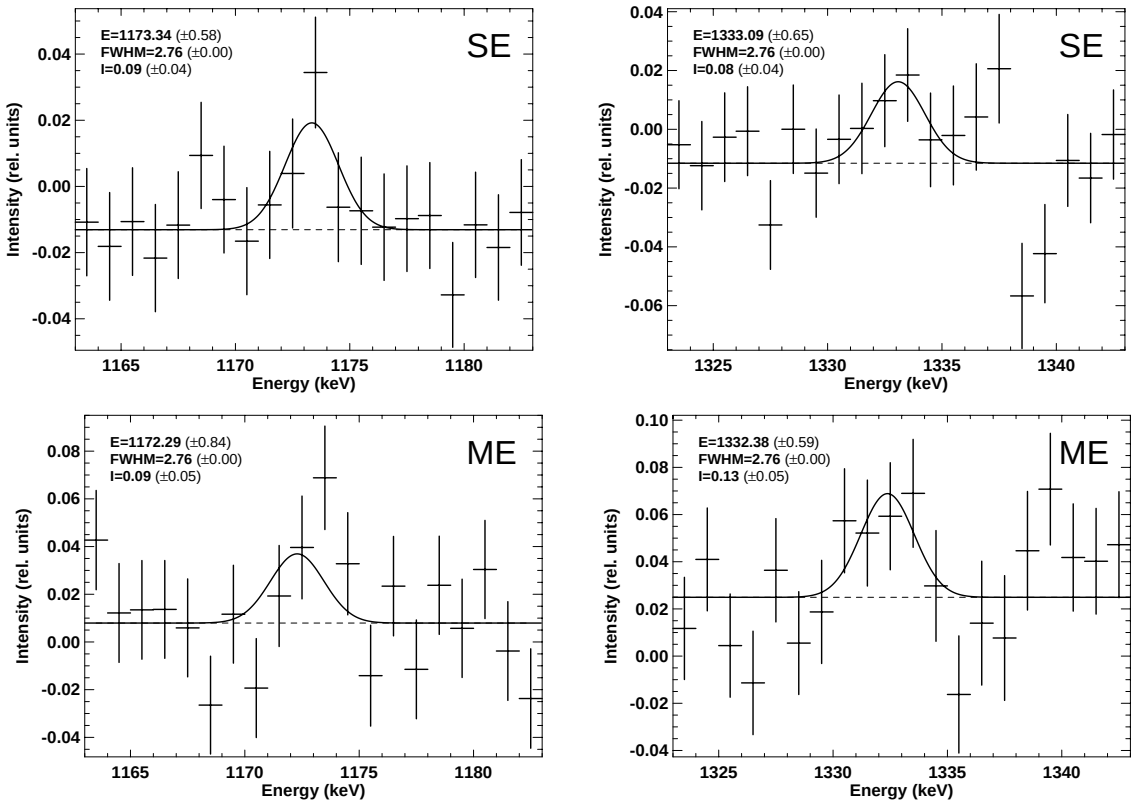

Figure 1. The spectra of two gamma-ray lines of ^{60}Fe from the Galaxy: 1173 keV and 1333 keV (both from SE and ME database). The data points are fitted with Gaussian profiles of fixed instrumental width (2.76 keV), and fixed continuum slope (flat). The line intensity is given in relative units (coefficients of the input sky map). For the SE database, we find the line flux is $(4.1 \pm 1.8) \times 10^{-5}$ph cm^{-2} s^{-1} *for 1173 keV line and* $(3.8 \pm 1.8) \times 10^{-5}$ph cm^{-2} s^{-1} *for 1333 keV line. For the ME database, the line flux is* $(4.1 \pm 2.4) \times 10^{-5}$ph cm^{-2} s^{-1} *for 1173 keV line and* $(5.9 \pm 2.4) \times 10^{-5}$ph cm^{-2} s^{-1} *for 1333 keV line.*

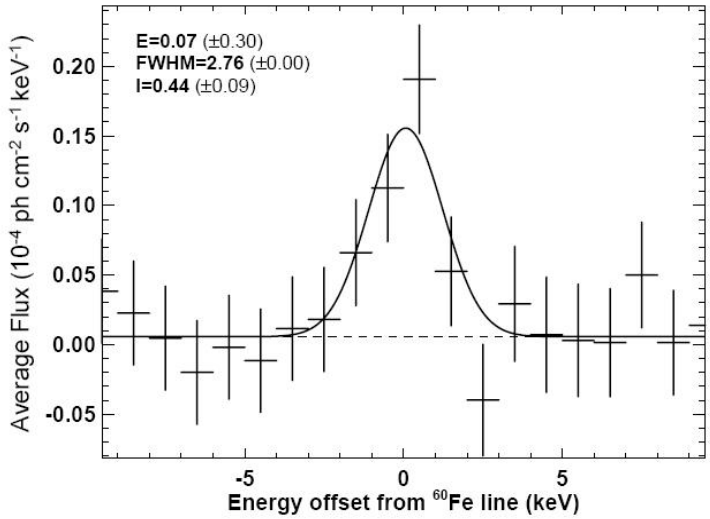

Figure 2. The combined spectrum of the ^{60}Fe signal in the Galaxy, superimposing the four spectra of Figure 1. In the laboratory, the line energies are 1173.23 and 1332.49 keV; here superimposed bins are zero at 1173 and 1333 keV. We find a detection significance of 4.9σ. The solid line represents a fitted Gaussian profile of fixed instrumental width (2.76 keV), and a flat continuum. The average line flux is estimated as $(4.4 \pm 0.9) \times 10^{-5}$ph cm^{-2} s^{-1}.

need a realistic model for these sources to derive correct spectra and line intensity. ^{26}Al and ^{60}Fe probably have similar production sites, related to massive stars and supernovae. In addition both of them are long-lived radioactive isotopes, so we have good reasons to believe their distributions correlate with each other well. We adopt the all sky distribution of ^{26}Al line from the 9-year COMPTEL observations [18] as the best model for the distribution of ^{60}Fe sources in the sky. We also have tried alternative sky maps: e.g. an exponential-disk model with scale radius 4 kpc, and scale height 180 pc. We find that different input sky maps do not change the line profiles and intensity significantly.

The combination of the four spectra of Fig. 1 is shown in Fig. 2. The line energies of the ^{60}Fe lines in the laboratory are 1173.23 and 1332.49 keV. For this superposition, we therefore define the zero on the energy axis at 1173 and 1333 keV, to derive the summed spectrum. The significance estimate for this combined spectrum is $\sim 4.9\sigma$. This improves the results from RHESSI [23] and the first year data of SPI [6]. The line flux estimated from the combined spectrum is $(4.4 \pm 0.9) \times 10^{-5}$ph cm^{-2} s^{-1}.

As another check, we have done the analyses on these observational data for the ^{26}Al line. We use the same data in a different energy band but with the same data selections from SPI orbits 17–359 and the same input sky map (the 9-year COMPTEL ^{26}Al map), applying model fitting for the SE case. This allows us to derive the flux ratio of ^{60}Fe/ ^{26}Al in a self-consistent way, which yields:

$$F(^{60}\mathrm{Fe})/F(^{26}\mathrm{Al}) = (14.8 \pm 6.0)\%. \qquad (2)$$

From the combined spectrum of ^{60}Fe lines, and an adopted ^{26}Al intensity of the SPI result from our earlier ^{26}Al studies [3], we obtain $F(^{60}\mathrm{Fe})/F(^{26}\mathrm{Al}) = (15.0 \pm 3.5)\%$.

5. SUMMARY AND DISCUSSIONS

In this paper, we report the results from 2.5 years of SPI observations of the ^{60}Fe decay lines in the Galaxy. The new measurements have detected both 1173 keV and 1333 keV lines of ^{60}Fe from the SE and ME databases. The combined spectrum of the four spectra lead to the detection of ^{60}Fe signals from the Galaxy with a significance of 4.9σ, which is better than the previous measurements. The average line flux of ^{60}Fe from the inner Galaxy region is $(4.4 \pm 0.9) \times 10^{-5}$ph cm^{-2} s^{-1}. From the same data and analysis applied to ^{26}Al, we found the flux ratio of ^{60}Fe/ ^{26}Al, $F(^{60}\mathrm{Fe})/F(^{26}\mathrm{Al}) = (14.8 \pm 6.0)\%$.

Because the ^{60}Fe signals are very weak, the individual spectral data points have large error bars, and we cannot determine line shape details. From the present data and fitting, it appears that a Gaussian with the width value of the instrumental resolution can fit the data well. This implies that the broadening of ^{60}Fe lines from astrophysical processes is not significant, which is also true of the ^{26}Al line. Most ^{60}Fe isotopes may be distributed in the interstellar medium with relatively normal turbulent velocities.

The theoretical predictions of the ratio of ^{60}Fe/ ^{26}Al have undergone changes in the last ten years.

Timmes et al. [26] calculated the ^{26}Al and ^{60}Fe nucleosynthesis in supernova explosions with models of chemical evolution and mass distribution in the interstellar medium, and predicted a flux ratio $F(^{60}\mathrm{Fe})/F(^{26}\mathrm{Al}) = 0.16 \pm 0.12$, which is consistent with our present SPI result. Since 2002, theoreticians have revised and updated the stellar nucleosynthesis models, including stellar rotation effects and improved stellar wind models, and revised nuclear reaction rates. The correspondingly revised flux ratio turned out to be 0.8 ± 0.4 [13], [19], [20], which would be inconsistent with our SPI result. Recently, Limongi & Chieffi [14] presented ^{26}Al and ^{60}Fe yields produced from their massive-star nucleosynthesis model by a generation of solar metallicity stars ranging in mass from $(11 - 120)M_{\odot}$, with the improved nuclear physics related to the nucleosynthesis of ^{26}Al and ^{60}Fe. Their calculations returned to a lower prediction of the ^{60}Fe/ ^{26}Al flux ratio of 0.185 ± 0.0625, which is again consistent with the observational constraints.

In summary, though large error bars and uncertainties exist, the original and the latest theoretical prediction of the flux ratio of ^{60}Fe/ ^{26}Al are consistent with the SPI result of this work. However, there are many problems calling for improvements both in observations and theories. For gamma-ray astronomy, more precise measurements of gamma-ray lines in the Galaxy are required, especially for the ^{60}Fe signals, which may require the more SPI data and the development of next-generation gamma-ray spectrometers/telescopes. Stellar evolution models have potential for improvements in processes related to the production of ^{60}Fe and ^{26}Al, e.g. convective layers in the inner stars, wind models for WR and O stars and the possible effects of stellar rotation [7]. More importantly, the nuclear physics still has serious uncertainties for the productions of ^{26}Al and ^{60}Fe. For example, the cross section of $^{12}\mathrm{C}(\alpha,\gamma)^{16}\mathrm{O}$ is uncertain, which affects the prediction of both ^{26}Al and ^{60}Fe; the situation of ^{60}Fe is strongly influenced by the cross sections of neutron capture and β-decay which are purely theoretical (also see Limongi & Chieffi [14]): no experimental data exist for the $^{59}\mathrm{Fe}(n,\gamma)$ and $^{60}\mathrm{Fe}(n,\gamma)$ rates, and their β^- decay depend on the temperature. Therefore, a concerted effort among stellar models, nucleosynthesis theory, and gamma-ray observations is required for a more satisfactory assessment of ^{60}Fe synthesis in the Galaxy.

ACKNOWLEDGMENTS

The INTEGRAL project is supported by government grants in all member states of the hardware teams. The SPI project has been completed under responsibility and leadership of CNES. We are grateful to ASI, CEA, CNES, DLR, ESA, INTA, NASA, and OSTC for support.

REFERENCES

[1] Attie, D. et al. 2003, A&A, 411, L71
[2] Chieffi, A. & Limongi, M. 2004, ApJ, 608, 405
[3] Diehl, R. et al. 2006, A&A, 449, 1025
[4] Halloin, H. et al. 2006, A&A, in preparation
[5] Hajdas, W. et al. 2003, A&A, 411, L43
[6] Harris, M.J. et al. 2005, A&A, 433, L49
[7] Hirschi, R., Meynet, G., Maeder, A. 2004, A&A, 425, 649
[8] Iyudin, A. F. et al. 1995, A&A, 300, 422
[9] Jensen, P.L. et al. 2003, A&A, 411, L7
[10] Knödlseder, J. et al. 1999, A&A, 344, 68
[11] Kurfess, J. D. et al. 1992, ApJ, 399, 137
[12] Leleux, P. et al. 2003, A&A, 411, L85
[13] Limongi, M. & Chieffi, A. 2003, ApJ, 592, 404
[14] Limongi, M. & Chieffi, A. 2006, ApJ, 647, 483
[15] Mahoney, W.A., Ling, J.C., Jacobson, A.S., & Lingerfelter, R.E. 1982, ApJ, 262, 742
[16] Matz, S.M. et al. 1988, Nature, 331, 416
[17] Murphy, D.C. & May, J. 1991, A&A, 247, 202
[18] Plüschke, S. et al. 2001, ESA-SP, 459, 55
[19] Prantzos, N. 2004, A&A, 420, 1033
[20] Rauscher, T., Herger, A., Hoffman, R.D. & Woosley, S.E. 2002, ApJ, 576, 323
[21] Renaud, M. et al. 2004, ESA-SP, 552, 81
[22] Roques, J.P. et al. 2003, A&A, 411, L91
[23] Smith, D.M. 2004, ESA-SP, 552, 45
[24] Strong, A.W. et al. 2005, A&A, 444, 495
[25] The, L.S. et al. 2006, A&A, 450, 1037
[26] Timmes, F.X. et al. 1995, ApJ, 449, 204